Astrophysics and Space Science manuscript No.
(will be inserted by the editor)

arXiv:astro-ph/0610955v1 31 Oct 2006

Andreas Reisenegger · Rodrigo Fernández · Paula Jofré

Internal heating and thermal emission from old neutron stars

Constraints on dense-matter and gravitational physics

Received: date / Accepted: date

Abstract The equilibrium composition of neutron star matter is achieved through weak interactions (direct and inverse beta decays), which proceed on relatively long time scales. If the density of a matter element is perturbed, it will relax to the new chemical equilibrium through non-equilibrium reactions, which produce entropy that is partly released through neutrino emission, while a similar fraction heats the matter and is eventually radiated as thermal photons. We examined two possible mechanisms causing such density perturbations: 1) the reduction in centrifugal force caused by spin-down (particularly in millisecond pulsars), leading to *rotochemical heating*, and 2) a hypothetical time-variation of the gravitational constant, as predicted by some theories of gravity and current cosmological models, leading to *gravitochemical heating*. If only slow weak interactions are allowed in the neutron star (modified Urca reactions, with or without Cooper pairing), rotochemical heating can account for the observed ultraviolet emission from the closest millisecond pulsar, PSR J0437-4715, which also provides a constraint on $|dG/dt|$ of the same order as the best available in the literature.

Keywords stars: neutron · dense matter · relativity · stars: rotation · pulsars: general · pulsars: individual (PSR B0950+08, PSR J0108−1431, PSR J0437−4715)

PACS 91.10.Op · 06.20.Jr · 97.60.Jd

A. Reisenegger and P. Jofré
Departamento de Astronomía y Astrofísica
Pontificia Universidad Católica de Chile
Casilla 306, Santiago 22, Chile
E-mail: areisene@astro.puc.cl;pdjofre@uc.cl

R. Fernández
Department of Astronomy & Astrophysics
University of Toronto
Toronto, ON M5S 3H8, Canada
E-mail: fernandez@astro.utoronto.ca

1 Introduction

Neutron star matter is composed of degenerate fermions of various kinds: neutrons (n), protons (p), electrons (e), probably muons (μ) and possibly other, more exotic particles. (We refer to electrons and muons collectively as leptons, l.) Neutrons are stabilized by the presence of other, stable fermions that block (through the Pauli exclusion principle) most of the final states of the beta decay reaction $n \rightarrow p + l + \bar{\nu}$. The large chemical potentials μ_i ($\approx$ Fermi energies) for all particle species i also make inverse beta decays, $p + l \rightarrow n + \nu$, possible. The neutrinos (ν) and antineutrinos ($\bar{\nu}$) leave the star without further interactions, contributing to its cooling (e. g., Shapiro & Teukolsky 1983; Yakovlev & Pethick 2004). The two reactions mentioned tend to drive the matter into a chemical equilibrium state, defined by $\eta_{npl} \equiv \mu_n - \mu_p - \mu_l = 0$.

If a matter element is in some way driven away from chemical equilibrium ($\eta_{npl} \neq 0$), free energy is stored, which is released by an excess rate of one reaction over the other. This energy is partly lost to neutrinos and antineutrinos (undetectable at present), and partly used to heat the matter. The heat is eventually lost as thermal (ultraviolet) photons emitted from the stellar surface.

The chemical imbalance can be caused by a change in the density of the stellar matter. This can in turn be produced in different ways. The first to be considered (by Finzi 1965; Finzi & Wolf 1968) was stellar pulsation; however, so far no clear evidence for this process has been seen. Gravitational collapse (Haensel 1992; Gourgoulhon & Haensel 1993) and mass accretion are also possible mechanisms, but in these contexts the non-equilibrium heating is probably overwhelmed by the energy released through other channels.

Here we review our work on neutron star heating through beta processes in two other contexts, which we consider to be the most promising in revealing information about the physics of dense matter and gravitation. One is *rotochemical heating* (Reisenegger 1995,

1997; Fernández & Reisenegger 2005, hereafter FR05; F
2006), in which the precisely measurable decrease of tl
stellar rotation rate, through the related reduction of tl
centrifugal force, makes the star contract progressivel
keeping it away from chemical equilibrium. The mo:
speculative *gravitochemical heating* is based on the h
pothesis that the gravitational “constant” may in fa
vary in time, causing a similar contraction or expansic
of the neutron star (Jofré et al. 2006, hereafter JRF06
We refer to our published papers for a detailed discussic
of our methods and formalism (see also Flores-Tulián &
2006). Here we restrict ourselves to a general, unifie
discussion of these two processes and their main impl
cations.

2 Time evolution

The formalism for calculating the evolution of the temperature and chemical imbalances for the case of rotochemical heating is described in § 2 of FR05. Here, we just outline the fundamental equations and the modifications required in order to treat the gravitochemical case as well. The evolution of the internal temperature, T, taken to be uniform inside the star, is given by the thermal balance equation,

$$\dot{T} = \frac{1}{C(T)}\left[L_H(\eta_{npl},T) - L_\nu(\eta_{npl},T) - L_\gamma(T)\right], \tag{1}$$

where C is the total heat capacity of the star, L_H is the total power released by the heating mechanism, L_ν the total power emitted as neutrinos, and L_γ the power released as thermal photons. Here and in what follows (including all figures), all temperatures, chemical imbalances, stellar radii, and luminosities are “redshifted” to the reference frame of a distant observer at rest with respect to the star.

The evolution of the chemical imbalances is given by

$$\begin{aligned}\dot{\eta}_{npl} = &-\left[A_{D,l}(\eta_{npe},T) + A_{M,l}(\eta_{npe},T)\right]\\ &-\left[B_{D,l}(\eta_{np\mu},T) + B_{M,l}(\eta_{np\mu},T)\right]\\ &-R_{npl}\Omega\dot{\Omega} + C_{npl}\dot{G}.\end{aligned} \tag{2}$$

The functions A and B quantify the effect of reactions towards restoring chemical equilibrium, and thus have the same sign of η_{npl} (FR05). The subscripts D and M refer to direct Urca reactions,

$$\begin{aligned} n &\longrightarrow p + l + \overline{\nu},\\ p + l &\longrightarrow n + \nu,\end{aligned} \tag{3}$$

which are possibly forbidden by momentum conservation, and modified Urca,

$$\begin{aligned} n + N &\longrightarrow p + N + l + \overline{\nu},\\ p + l + N &\longrightarrow n + N + \nu,\end{aligned} \tag{4}$$

where an aditional nucleon N must participate in order to conserve momentum (e. g., Shapiro & Teukolsky 1983; Yakovlev & Pethick 2004). The scalars R_{npl} and C_{npl} quantify the departure from equilibrium due to the changes in the centrifugal force ($\propto \Omega\dot{\Omega}$) and the gravitational constant ($\dot{G}$), being positive and depending on the stellar model and equation of state (FR05; Reisenegger et al. 2006; JRF06).

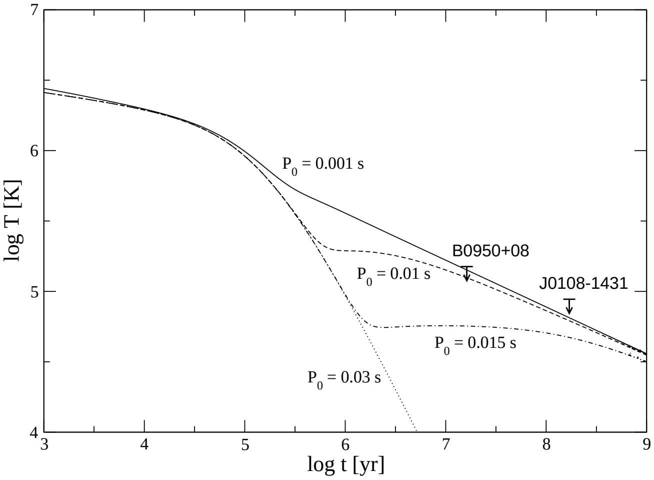

Fig. 1 Predicted time-evolution of the surface temperature, T_s, of a neutron star with rotochemical heating. All curves correspond to stars with mass $M = 1.4\ M_\odot$, equation of state A18+δv+UIX* (Akmal et al. 1998), which allows only modified Urca processes to occur, and magnetic dipole spin-down with $B_{\rm dipole} = 2.5 \times 10^{11}$ G. Each curve is labeled by the assumed initial rotation period. The upper limits correspond to observational constraints for pulsars B0950+08 (Zavlin & Pavlov 2004) and J0108−1431 (Mignani et al. 2003, as interpreted by Kargaltsev et al. 2004), both of which have magnetic dipole field strengths very close to the assumed value.

Figure 1 shows the solution of the coupled differential equations 1 and 2 for the evolution of a classical pulsar with a moderate magnetic field and different assumed initial rotation periods under pure rotochemical heating ($\Omega\dot{\Omega} < 0$, $\dot{G} = 0$). It can be seen that, for very fast initial rotation, the pulsar can be kept warm beyond the standard cooling time of $\sim 10^7$ yr, at a level that is close to current observational constraints.

The case of a “millisecond pulsar” (a neutron star with fast rotation and a weak magnetic dipole field) is illustrated in Figure 2. It first cools down from its high birth temperature, while the chemical potential imbalances η_{npl} slowly increase due to the decreasing rotation rate, until rotochemical heating increases the temperature again, and the reactions stop the rise of the chemical potential imbalances.

3 Stationary state

If the relevant forcing ($\Omega\dot{\Omega}$ or $\dot{G}$) changes slowly with time, the star eventually arrives at a stationary state, where the rate at which the equilibrium concentrations

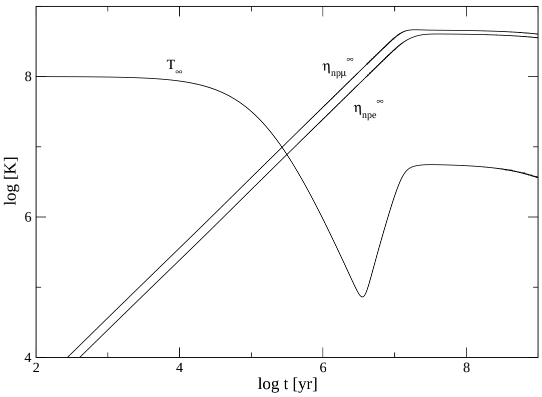

Fig. 2 (taken from FR05) Evolution of the internal temperature and chemical imbalances under the rotochemical heating effect for a $1.4M_\odot$ star calculated with the A18 + $\delta\upsilon$ + UIX* equation of state (Akmal et al. 1998), with initial temperature $T = 10^8$ K, null initial chemical imbalances, and magnetic dipole spin-down with field strength $B = 10^8$ G and initial period $P_0 = 1$ ms.

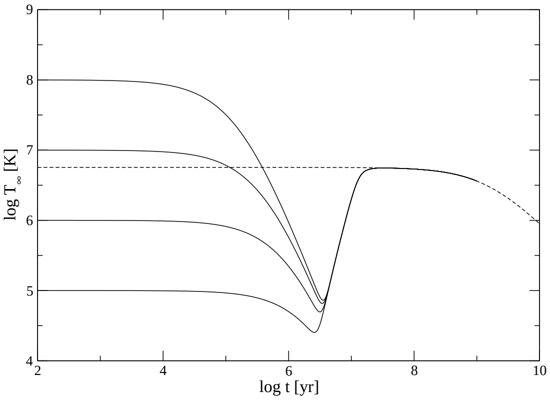

Fig. 3 (from FR05) Evolution of the internal temperature under rotochemical heating for different initial temperatures. We set $\eta_{npe} = \eta_{np\mu} = 0$. The short-dashed line is the quasi-equilibrium solution, obtained by solving $\dot{T} = 0$ and $\dot{\eta}_{npe} = \dot{\eta}_{np\mu} = 0$. The stellar model and spin-down parameters are the same as in Figure 2.

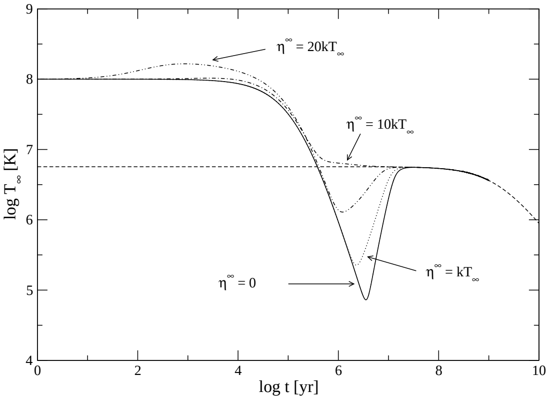

Fig. 4 (from FR05) Evolution of the internal temperature under rotochemical heating for different initial chemical imbalances $\eta_{npe} = \eta_{np\mu} \equiv \eta$ and the same initial temperature $T = 10^8$ K at $t = 0$. The line styles, the stellar model, and the spin-down parameters are the same as in Figure 3.

are modified by this forcing is the same as that at which the reactions drive the system toward the new equilibrium configuration, with heating and cooling balancing each other (Reisenegger 1995). The evolution to this state for pure rotochemical heating is illustrated in Figure 2. Figures 3 and 4 show that the state reached is independent on the assumed initial conditions.

The properties of this stationary state can be obtained by the simultaneous solution of equations (1) and (2) with $\dot{T} = \dot{\eta}_{npl} = 0$. The existence of the stationary state makes it unnecessary to model the full evolution of the temperature and chemical imbalances of the star in order to calculate the final temperature, since the stationary state is independent of the initial conditions (see FR05 for a detailed analysis of the rotochemical heating case). For given values of $\Omega\dot{\Omega}$ and $\dot{G}$, it is thus possible to calculate the temperature of an old pulsar that has reached the stationary state, without knowing its exact age.

When only modified Urca reactions operate, it is possible to solve analytically for the stationary values of the photon luminosity L_γ^{st} and chemical imbalances η_{npl}^{st}, as a function of stellar model and current value of $\Omega\dot{\Omega}$ and $\dot{G}$. The reason for this is that the longer equilibration timescale given by the slower modified Urca reactions yields stationary chemical imbalances satisfying $\eta_{npl} \gg kT$. In this limit, the term $L_H - L_\nu$ in the thermal balance equation can be written as $K_{Le}\eta_{npe}^8 + K_{L\mu}\eta_{np\mu}^8$, where $K_{L,l}$ are positive constants that depend only on stellar mass and equation of state (FR05; JRF06). For typical equations of state, the photon luminosity in the stationary state is

$$L_\gamma^{st} \simeq 10^{30-31} \left| \frac{\dot{P}_{-20}}{P_{\rm ms}^3} + \frac{\dot{G}/G}{3 \times 10^{-11}\ \ {\rm yr}^{-1}} \right|^{8/7} {\rm erg\ s}^{-1}, \quad (5)$$

where $P_{\rm ms}$ is the rotation period in milliseconds, and $\dot{P}_{-20}$ is its time derivative in units of 10^{-20} (dimensionless), and the effective surface temperature of the star in the stationary state is

$$T_s^{st} \simeq (2-3) \times 10^5 \left| \frac{\dot{P}_{-20}}{P_{\rm ms}^3} + \frac{\dot{G}/G}{3 \times 10^{-11}\ \ {\rm yr}^{-1}} \right|^{2/7} {\rm K}. \quad (6)$$

Finally, the timescale for the system to reach the stationary state is

$$\tau_{st} \simeq 2 \times 10^7 \left| \frac{\dot{P}_{-20}}{P_{\rm ms}^3} + \frac{\dot{G}/G}{3 \times 10^{-11}\ \ {\rm yr}^{-1}} \right|^{-6/7} {\rm yr}. \qquad (7)$$

4 Comparison to observations

In order to verify this model and constrain the value of $|\dot{G}/G|$, we need a neutron star that (1) has a measured surface temperature (or at least a good enough upper limit on the latter), and (2) is confidently known to be older than the timescale to reach the stationary state. So far, the only object satisfying both conditions is the millisecond pulsar closest to the Solar System, PSR J0437-4715 (hereafter J0437), whose surface temperature was inferred from an HST-STIS ultraviolet observation by Kargaltsev et al. (2004). Its spin-down age, $\tau_{\rm sd} \simeq 5 \times 10^9$ yr (e.g., van Straten et al. 2001), and the cooling age of its white dwarf companion, $\tau_{\rm WD} \simeq (2.5-5.3) \times 10^9$ yr (Hansen & Phinney 1998), are much longer than the time required to reach the steady state for both rotochemical and gravitochemical heating, in the latter case under the condition that $|\dot{G}/G| \geq 10^{-13}$ yr^{-1}.

Consequently, we consider stellar models constructed from different equations of state, with masses satisfying the constraint obtained for J0437 by van Straten et al. (2001), $M_{\rm psr} = 1.58 \pm 0.18 M_\odot$, and calculate the stationary temperature for each. Figure 5 compares the predictions for the case of pure rotochemical heating with the measured spin-down parameters of J0437 (for various equations of state and neutron star masses) to the temperature inferred from the observation of Kargaltsev et al. (2004).

In Figure 6, we compare the same observational constraints on the temperature of this pulsar to the theoretical predictions for pure gravitochemical heating, assuming $|\dot{G}/G| = 2 \times 10^{-10}$ yr^{-1}. As can be seen, this value is such that the stationary temperatures of all stellar models lie just above the 90 % confidence contour, and therefore represents a rather safe and general upper limit.

When the stellar mass becomes large enough for the central pressure to cross the threshold for direct Urca reactions, T_s drops abruptly, due to the faster relaxation towards chemical equilibrium. This occurs in two steps, as electron and muon direct Urca processes have different threshold densities (see, e.g., FR05). Conventional neutron star cooling models reproduce observed temperatures better when only modified Urca reactions are considered (e. g., Yakovlev & Pethick 2004; Page 2006). Restricting our sample to the equations of state that allow only modified Urca reactions in the mass range considered here, namely $A18 + \delta v$, $A18 + \delta v+$ UIX, BPAL21, and BPAL31, we obtain a more restrictive upper limit on $|\dot{G}|$, as shown in Figure 7, yielding $|\dot{G}/G| < 4 \times 10^{-12}$ yr^{-1}.

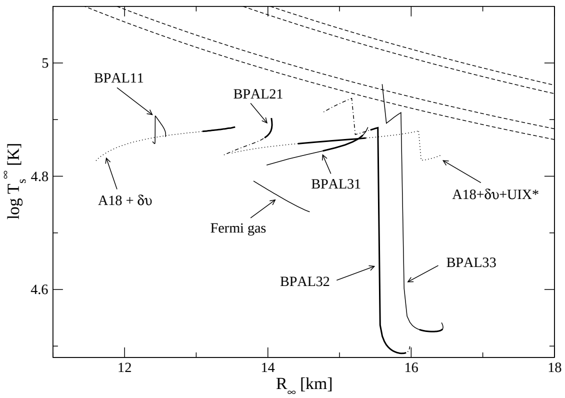

Fig. 5 (taken from FR05) Surface temperature due to rotochemical heating in the stationary state as function of stellar radius for different equations of state, shown as solid lines (APR from Akmal et al. 1998 and BPAL from Prakash et al. 1988), for the spin parameters of PSR J0437-4715. Dashed lines are 68% and 90% confidence contours of the blackbody fit to the emission from this pulsar (Kargaltsev et al. 2004). Bold lines indicate, for each equation of state, the mass range allowed by the constraint of van Straten et al. (2001), $M_{PSR} = 1.58 \pm 0.18 M_\odot$. BPAL32 and BPAL33 allow direct Urca reactions in the observed mass range of PSR J0437.

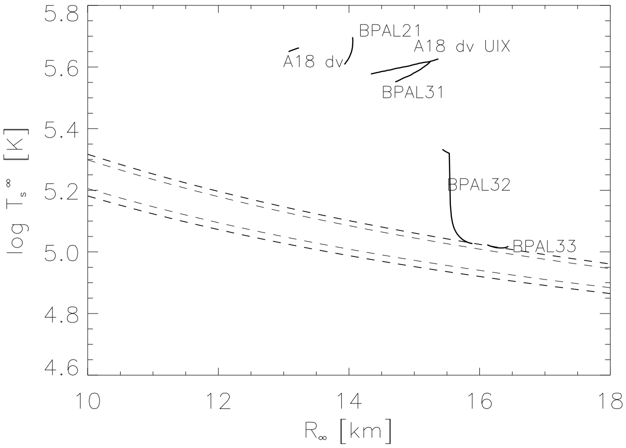

Fig. 6 (from JRF06) Surface temperature due to gravitochemical heating in the stationary state as function of stellar radius for different equations of state. The value of $|\dot{G}/G| = 2 \times 10^{-10}$ yr^{-1} is chosen so that all stationary temperature curves lie above the observational constraints. Otherwise, the meanings of lines and symbols are as in Figure 5.

5 Discussion and Conclusions

5.1 Rotochemical heating

Using the equations of state that allow only modified Urca reactions within the allowed mass for PSR J0437-

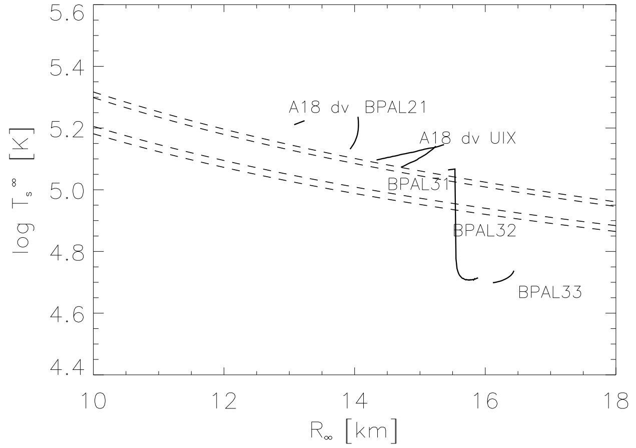

Fig. 7 (from JRF06) Same as Figure 6, but now the value of $|\dot{G}/G| = 4 \times 10^{-12}$ yr^{-1} is chosen such that only the stationary temperature curves with modified Urca reactions are above the observational constraints.

4715, rotochemical heating predicts an effective temperature in the narrow range $T_{s,eq} = (6.9\text{–}7.9) \times 10^4$ K, about 20% lower than the blackbody fit of Kargaltsev et al. (2004). There are three possible reasons why the prediction does not quite match the observation:

1. We are not taking superfluidity into account. This would reduce Urca reaction rates, lengthening the equilibration timescale and raising the stationary-state temperature (Reisenegger 1997).
2. We are neglecting other heating mechanisms (some of them directly related to superfluidity), which could further raise the temperature at any stage in the thermal evolution. Nonetheless, in millisecond pulsars, all proposed mechanisms appear to be less important than rotochemical heating (Schaab et al. 1999; Kargaltsev et al. 2004).
3. The thermal spectrum could deviate from a blackbody, as for the isolated neutron star RX J1856-3754, which has a well-determined blackbody X-ray spectrum that underpredicts the optical flux (Walter & Matthews 1997), indicating a more complex spectral shape of its thermal emission.

Kargaltsev et al. (2004) stress that PSR J0437-4715 has a higher surface temperature than the upper limit for the younger, "classical" pulsar J0108-1431, $T_s < 8.8 \times 10^4$ K, inferred from the optical non-detection by Mignani et al. (2003) and shown in our Figure 1. In the rotochemical heating model, these two pulsars are in very different regimes: J0437 is in the stationary state in which its temperature can be predicted from its spin-down parameters, whereas J0108 has a 680 times smaller spin-down power ($\propto \Omega\dot{\Omega}$), and will therefore not reach a detectable stationary state. Its equilibration timescale, according to equation (7), is 2×10^{11} yr, longer than the age of the Universe and certainly much longer than the spin-down age of the pulsar. Thus, its heat content (if any) is due to its earlier, faster rotation, which may have built up a significant chemical imbalance that is currently being decreased by ongoing reactions in its interior (see Fig. 1). Depending on its initial rotation period, its surface temperature may be substantially smaller than both J0437's observed temperature and its own current upper limit.

5.2 Gravitochemical heating

Table 1 lists some of the many experiments performed so far to test the constancy of G (see Uzan 2003 and Will 2006 for recent reviews). The second column contains the upper limits on its time variation, most usefully expressed as $|\dot{G}/G|$, and the third is a rough time scale over which each experiment is averaging this variation. Based on the latter, the experiments can be separated into three classes. The first two experiments on the list measure the variation of G from the early Universe to the present time, and the constraint on the present-day value of $|\dot{G}/G|$ is based on assuming a time dependence $G(t) \propto t^{-\alpha}$, where t is the time since the Big Bang, and α is a constant constrained by these experiments. The next four are sensitive to variations over long timescales, 10^{9-10} yr, but without reaching into the very early Universe. The last four experiments measure the change of G directly over short, "human" timescales of years or few decades. Even though results from the first category are nominally the most restrictive on a long-term variation of G, they depend crucially on the assumed form of the variation of G near the Big Bang. Thus, it is still useful to consider measurements of the second and third categories, which could directly detect variations of G in more recent times.

The new method advocated here, namely gravitochemical heating of neutron stars, falls closest to the second category, as its timescale is much longer than human, but does not reach into the early Universe. However, it probes somewhat shorter timescales than the other methods in this category. In the most general case, when direct Urca reactions are allowed to operate, we obtain an upper limit $|\dot{G}/G| < 2 \times 10^{-10}$ yr^{-1}. Restricting the sample of equations of state to those that allow only modified Urca reactions, we obtain a much more restrictive upper limit, $|\dot{G}/G| < 4 \times 10^{-12}$ yr^{-1} on a time scale $\sim 10^8$ yr (the time for the neutron star to reach its quasi-stationary state), competitive with constraints obtained from the other methods probing similar timescales. However, since the composition of matter above nuclear densities is uncertain and millisecond pulsars are generally expected to be more massive than classical pulsars, we cannot rule out the result for the direct Urca regime.

Further progress in our knowledge of neutron star matter will allow this method to become more effective at constraining variations in G. The method can also be improved with an increased sample of objects with measured thermal emission or good upper limits.

Table 1 Previous upper bounds on $|\dot{G}/G|$.

Method	$\vert\dot{G}/G\vert_{\max}$ [10^{-12} yr^{-1}]	Time scale [yr]	Reference
Big Bang Nucleosynthesis	0.4	1.4×10^{10}	Copi et al. (2004)
Microwave background	0.7	1.4×10^{10}	Nagata et al. (2004)
Globular cluster isochrones	35	10^{10}	Degl'Innocenti et al. (1996)
Binary neutron star masses	2.6	10^{10}	Thorsett (1996)
Helioseismology	1.6	4×10^{9}	Guenther et al. (1998)
Paleontology	20	4×10^{9}	Eichendorf & Reinhardt (1977)
Lunar laser ranging	1.3	24	Williams et al. (2004)
Binary pulsar orbits	9	8	Kaspi et al. (1994)
White dwarf oscillations	250	25	Benvenuto et al. (2004)

Acknowledgements We thank G. Pavlov and O. Kargaltsev for letting us know about their work in advance of publication and for kindly providing their data in electronic form. The authors are also grateful to C. Dib, O. Espinosa, S. Flores-Tulián, M. Gusakov, E. Kantor, R. Mignani, D. Page, M. Taghizadeh, and M. van Kerkwijk for discussions that benefited the present paper. This work made use of NASA's Astrophysics Data System Service, and received financial support from FONDECYT through regular grants 1020840 and 1060644.

References

Akmal, A., Pandharipande, V. R., & Ravenhall, D. G. 1998, Phys. Rev. C, 58, 1804
Benvenuto, O., García-Berro, E., & Isern, J. 2004, Phys. Rev. D, 69, 2002
Brans, C., & Dicke, R. H. 1961, Phys. Rev., 124, 925
Copi, C., Davis, A., & Krauss, L. 2004, Phys. Rev. Lett., 92, 17
Degl'Innocenti, S. et al. 1996, Astron. Astrophys., 312, 345
Dirac, P. 1937, Nature, 139, 323
Eichendorf, W. & Reinhardt, M. 1977, Mitteilungen der Astronomischen Gesellschaft Hamburg, 42, 89 (result cited in Uzan 2003)
Fernández, R., & Reisenegger, A. 2005, Astrophys. J., 625, 291: FR05
Finzi, A. 1965, Phys. Rev. Lett., 15, 599
Finzi, A., & Wolf, R. A. 1968, Astrophys. J., 153, 835
Flores-Tulián, S., & Reisenegger, A. 2006, Mon. Not. R. Astron. Soc., 372, 276
Gourgoulhon, E., & Haensel, P. 1993, Astron. Astrophys., 271, 187
Guenther, D. B., Krauss, L. M., & Demarque, P. 1998, Astrophys. J., 498, 871
Haensel, P. 1992, Astron. Astrophys., 262, 131
Jofré, P., Reisenegger, A., & Fernández, R. 2006, Phys. Rev. Lett., 97, 131102: JRF06
Hansen, B. M. S., & Phinney, E. S. 1998, Mon. Not. R. Astron. Soc., 294, 569
Kargaltsev, O., Pavlov, G. G., & Romani, R. 2004, Astrophys. J., 602, 327
Kaspi, V. M., Taylor, J. H., & Ryba, M. F. 1994, Astrophys. J., 428, 713
Mignani, R. P., Manchester, R. N., & Pavlov, G. G. 2003, Astrophys. J., 582, 978
Nagata, R., Chiba, T., & Sugiyama, N. 2004, Phys. Rev. D, 69, 3512
Page, D. 2006, these Proceedings
Prakash, M., Ainsworth, T. L., & Lattimer, J. M. 1988, Phys. Rev. Lett., 61, 2518
Reisenegger, A. 1995, Astrophys. J., 442, 749
Reisenegger, A. 1997, Astrophys. J., 485, 313
Reisenegger, A., Jofré, P., Fernández, R., & Kantor, E., Astrophys. J., in press (astro-ph/0606322)
Schaab, Ch., Sedrakian, A., Weber, F., & Weigel, M. K. 1999, Astron. Astrophys., 346, 465
Shapiro, S. L., & Teukolsky, S. A. 1983, Black Holes, White Dwarfs, and Neutron Stars (New York: Wiley)
Thorsett, S. E. 1996, Phys. Rev. Lett., 77, 1432
Uzan, J. 2003, Rev. Mod. Phys., 75, 403
van Straten, W., et al. 2001, Nature, 412, 158
Walter, F. M., & Matthews, L. D. 1997, Nature, 389, 358
Will, C. 2006, Living Reviews in Relativity, 9, 3
Williams, J. G., Turyshev, S. G., & Boggs, D. H. 2004, Phys. Rev. Lett., 93, 261101-1-4
Yakovlev, D. G., & Pethick, C. J. 2004, Ann. Rev. Astron. Astrophys., 42, 169
Zavlin, V. E., & Pavlov, G. G. 2004, Astrophys. J., 616, 452